IOP Publishing Journal of Physics D: Applied Physics

J. Phys. D: Appl. Phys. **54** (2021) 505501 (12pp) https://doi.org/10.1088/1361-6463/ac2110

# A proposal to enhance SnS solar cell efficiency: the incorporation of SnSSe nanostructures

**Maykel Courel[1,*], P Beltrán-Bobadilla[1], F J Sánchez-Rodríguez[2], I Montoya De Los Santos[3], M Ojeda[1], A Carrillo-Osuna[2], Hugo J Cortina-Marrero[3], L Hechavarría-Difur[3], L M Pérez[4], D Laroze[4] and E Feddi[5]**

[1] Centro Universitario de los Valles. Universidad de Guadalajara, Carretera Guadalajara—Ameca Km. 45.5, C.P. 46600 Ameca, Jalisco, Mexico
[2] Facultad de Ciencias Físico-Matemáticas, Universidad Autónoma de Sinaloa, C.P. 80010 Culiacán, Sinaloa, Mexico
[3] Instituto de Estudios de la Energía, Universidad del Istmo, C.P. 70760 Santo Domingo Tehuantepec, Oaxaca, Mexico
[4] Instituto de Alta Investigación, CEDENNA, Universidad de Tarapacá, Casilla 7D, Arica, Chile
[5] Group of Optoelectronic of Semiconductors and Nanomaterials, ENSAM, Mohammed V University in Rabat, Rabat, Morocco

E-mail: maykel.courel@academicos.udg.mx

Received 30 April 2021, revised 19 July 2021
Accepted for publication 25 August 2021
Published 28 September 2021

**Abstract**

Tin sulfide (SnS) semiconductor has recently attracted a great deal of attention from the scientific community regarding its application in solar cells. However, SnS solar cell efficiencies are still limited to less than 5%. The incorporation of nanostructures into solar cells has been demonstrated to be a potential route to improve device performance. So far, there have been no reports on the incorporation of nanostructures into SnS solar cells. In this work, a theoretical study on the incorporation of tin sulfide selenide (SnSSe) nanostructures in the form of quantum wells (QWs) into SnS solar cells under the radiative limit is presented, for the first time. In particular, the impact of well number, well thickness, and Se/(S + Se) compositional ratio at the wells, on solar cell characteristics, is evaluated. An efficiency enhancement of 11.1% is found for a SnS/SnSSe QW solar cell, compared to the optimized device without nanostructures, for 50 wells of 54 nm width with a Se/(S + Se) well composition of 0.4 and considering barrier thicknesses of 5 nm, which is a result of the increase in short-circuit current density of 14.5%. The influence of defects at wells and barriers, as well as defects at interfaces, on solar cell behavior is also presented, demonstrating that the introduction of QWs can result in higher efficiencies than that of the device without nanostructures. In this sense, the addition of SnSSe nanostructures to SnS solar cells is introduced as a potential route to promote the absorption of photons with energy lower than the SnS band-gap, while keeping open-circuit voltage values similar to those of a SnS solar cell without nanostructures, thereby increasing solar cell efficiency.

Keywords: SnS solar cells, solar cell modeling, quantum wells, radiative and non-radiative recombination

(Some figures may appear in colour only in the online journal)

* Author to whom any correspondence should be addressed.

 © 2021 IOP Publishing Ltd Printed in the UK

## 1. Introduction

Tin sulfide (SnS) is a potential candidate for the next generation of solar cells [1]. This semiconductor is described by a p-type conductivity, with a band-gap value near 1.3 eV with direct transitions, and consequently a high absorption coefficient [1–4]. However, SnS solar cell efficiencies remain lower than 5% [5–7], making it necessary to analyse new strategies to improve the device performance. One of the main problems affecting the first and second generations of solar cells is the inability to absorb photons with energies lower than the bulk semiconductor band-gap. The absorption of photons with energies lower than the bulk band-gap would increase the current density of the device and, consequently, the solar cell efficiency if the output voltage of the cells was not drastically degraded. This goal cannot be achieved by merely changing the semiconductor band-gap. Despite the fact that lower band-gap values guarantee a higher absorption of photons, an increase in recombination is also found, thereby degrading the output voltage of the solar cells and, in turn, efficiency. In this sense, it is important to find a new configuration that guarantees higher absorption of photons with the lowest reduction of the output voltage of the cells.

The addition of nanostructures such as quantum wells (QWs) to bulk material has been shown to be a potential route to improve device efficiency since it allows the absorption of extra photons with energies lower than the bulk band-gap [8–11]. That is, when QWs are embedded within an absorber material so that a type I band-alignment is formed, the quantum confinement allows the formation of discretized energy levels, extending the light absorption domain to energies lower than that of the absorber band-gap. In fact, by controlling the width and depth of wells, the absorption of photons can be tailored to achieve a maximum value [12, 13]. In this sense, the inclusion of QWs in solar cells would result in short-circuit current density ($J_{sc}$) values higher than that of solar cells without nanostructures, and thereby higher efficiencies, if open-circuit voltage ($V_{oc}$) were not drastically reduced. However, the addition of QWs can also increase carrier losses due to quantum confinement, thereby reducing the $V_{oc}$ of the cell, which is necessary to study conditions under which carrier generation overcomes losses due to recombination.

QW solar cells (QWSCs) have received a great deal of attention from the scientific community since their proposal in 1990 [11]. QWSCs based on different compounds have been studied to achieve efficiencies higher than the ones obtained in solar cells without the inclusion of wells [8–13]. The addition of tin sulfide selenide (SnSSe) nanostructures in the form of QWs into SnS material constitutes a potential solution to the problem of low solar cell efficiency values. The SnSSe compound can be obtained by the partial substitution of S by Se atoms, with a direct band-gap variation from 1.3 eV corresponding to SnS material [1, 14, 15] to 1.0 eV corresponding to tin selenide (SnSe) material [14, 16] as a function of Se incorporation into the lattice [15]. In addition, an interesting characteristic is the formation of a type I band-alignment in the SnS/SnSSe heterostructure with a conduction band offset given by the difference in band-gap of SnS and SnSSe materials, and consequently there is no valence band discontinuity, as experimentally reported [17]. Therefore, photons with energy in the range of 1.0–1.3 eV can be absorbed in SnS/SnSSe QWSC depending on Se composition and SnSSe well thickness, enhancing the $J_{sc}$ of the solar cell in comparison with the SnS solar cell without SnSSe nanostructures, while keeping $V_{oc}$ values near to the ones of SnS, in turn increasing solar cell efficiency. So far, information is lacking on the application of SnSSe nanostructures in solar cells. Only a few works have reported the application of SnSe nanostructures as a counter electrode in dye-sensitized solar cells, with a maximum conversion efficiency, $J_{sc}$, $V_{oc}$ and fill factor (FF) values of 5.52%, 10.38 mA cm$^{-2}$, 760 mV, and 70%, respectively [18]. In this sense, this type of study is only just beginning. In particular, there are neither theoretical nor experimental studies on the application of SnSSe QWs in SnS solar cells. In this work, the addition of SnSSe QWs into SnS solar cells is theoretically evaluated under the radiative and nonradiative limit for the first time. In particular, conditions that allow QWSC efficiencies greater than that of optimized SnS solar cells without QWs are presented and discussed.

## 2. Theoretical considerations

### 2.1. Calculations under the radiative limit

The addition of SnSSe QWs into SnS solar cells is evaluated in this work for the first time. In particular, numerical calculations on SnS/SnSSe QWSCs are firstly performed under the radiative limit, where only band-to-band transitions are considered. QWs are commonly implemented into the intrinsic region of a p–i–n structure; therefore, it is considered that the SnSSe compound is described by a low intrinsic defect formation providing an almost intrinsic nature in the absence of doping. This consideration would guarantee the intrinsic nature of both SnS barrier and SnSSe well materials. In the first step, conditions that allow the maximum efficiencies in SnS and SnSe solar cells are studied for comparison. The radiative limit constitutes an important first step to survey the potential application of an absorber material into solar cells. This limit only considers losses due to band-to-band transitions and consequently, losses from bulk and interface defects, surface reflection, and series and shunt resistances are neglected. Under the radiative limit, an ideal buffer layer is also considered so that most photons can be absorbed in the intrinsic region formed by SnS/SnSSe QWs. In addition, it is assumed that all photogenerated electron–hole pairs within the absorber material that do not recombine contribute to the photocurrent. It is important to point out that the purpose of this first study is to find conditions that allow maximum efficiency in the proposed device.

Solar cell parameters can be obtained from $J$–$V$ characteristics. For SnS and SnSe solar cells under the radiative limit, the $J$–$V$ characteristics can be evaluated by the following equation [19]:

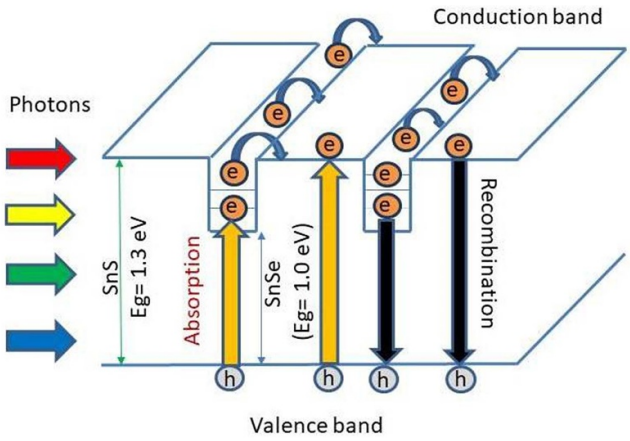



**Figure 1.** Sketch diagram of SnS solar cell with the inclusion of SnSe quantum wells. Absorption and recombination processes are illustrated.

$$J = qWn_i^2 B\left[\exp\left(\frac{qV}{kT}\right) - 1\right] - J_{PH} \tag{1}$$

where $q$ is the electron charge, $W$ is the absorber thickness, $n_i$ is the intrinsic carrier concentration, and $B$ is the radiative coefficient of SnS or SnSe material, this latter being determined from the detailed balance theory. Besides, $V$ is the terminal voltage, $kT$ is the thermal energy and $J_{PH}$ is the photocurrent density. The first term of equation (1) is associated with optical losses (radiative recombination) and the second term with the photocurrent due to optical generation. For the optical generation calculation, the absorption coefficient is calculated while for optical losses, the radiative coefficient should be evaluated. Details on radiative coefficient and photocurrent density calculations can be found in a previous paper [19].

In the second step, the inclusion of SnSSe QWs into SnS absorber material is considered. The particular case of SnSe QWs with a band-gap of 1.0 eV within SnS host material with a band-gap of 1.3 eV is presented in figure 1. For QWSCs, calculations are also firstly performed under the radiative limit. Two opposite processes take place in solar cells, the first one is the absorption of photons and the second one is the recombination of photogenerated carriers at both barriers and wells, as illustrated in figure 1. At wells, absorption and recombination processes take place through discrete levels. The Schrödinger equation is used under the framework of the effective mass approximation and with the Ben–Daniel–Duke boundary conditions to calculate eigenvalues at wells as functions of well thickness and depth. After this, generation and recombination rates can be calculated, thereby evaluating the $J$–$V$ characteristics of QWSCs by the following equation [8]:

$$\begin{aligned} J_{QWSC} = {} & qWn_i^2 B \\ & \times \left\{1 + f_w\left[\gamma_B \gamma_{DOS}^2 \exp\left(\frac{\Delta Eg - qFL_W}{kT}\right) - 1\right]\right\} \\ & \times \left[\exp\left(\frac{qV}{kT}\right) - 1\right] - J_{PH} \end{aligned} \tag{2}$$

where $f_w$ is the fraction of the SnS region filled with QWs, $\gamma_B$ is defined as the ratio between the radiative recombination coefficient of wells and the barrier, $\gamma_{DOS} = g_W/g_b$ is the density of states enhancement factor with $g_W$ and $g_b$ as the effective density of states of wells and barrier, respectively. In addition, $\Delta E_g = Eg_b - Eg_w$, where $Eg_b$ and $Eg_w$ are the band-gap energy of barrier and well, respectively, $F$ is the electric field at the absorber depletion layer and $L_W$ is the well thickness. For QWSCs, the photocurrent density is given by:

$$J_{PH} = q\int F(\lambda)\left[1 - \exp\left(-\alpha_b W - \alpha_W N L_W\right)\right] d\lambda \tag{3}$$

where $F(\lambda)$ is the number of photons as a function of wavelength taken from the AM1.5G solar spectrum, $\alpha_b$ and $\alpha_W$ are the absorption coefficient of barrier and well, respectively, and $N$ is the number of wells. The absorption coefficients of host material and wells were evaluated from expressions reported in the literature [19, 20]. In the case of well material, both absorption coefficient and effective density of states are stepped functions dependent on energy eigenvalues obtained from solving the Schrödinger equation. It is important to point out that photogenerated electrons within the wells should escape from wells to contribute to the current of the device. A photocarrier extraction probability given by the competition between the escape lifetime ($\tau_e$) and recombination lifetime ($\tau_r$) of carriers within the QW is evaluated by [21]:

$$\eta = \frac{\dfrac{1}{\tau_e}}{\dfrac{1}{\tau_e} + \dfrac{1}{\tau_r}} \tag{4}$$

where carrier lifetime can be obtained from the recombination mechanism assumed (radiative or nonradiative), while escape lifetime is evaluated taking into account the contribution of thermionic emission and tunneling mechanism supported by the electric field, as reported in [21]. In particular, in some cases, a photocarrier extraction probability of near 1 for room temperature was found. This means that most photogenerated carriers are able to escape from wells assisted by tunneling and thermionic processes.

For evaluating the radiative coefficient in bulk, barriers, and wells, an expression is obtained from the detailed balance theory as follows:

$$B = \frac{8\pi n_r^2}{c^2 h^3 n_i^2}\int_{E_1}^{\infty} \frac{\alpha E^2 dE}{\exp\left(\frac{E}{kT}\right) - 1} \tag{5}$$

where $h$ is Planck's constant, $c$ is the speed of light, $E_1$ is either the band-gap in the bulk and barrier material or the effective band-gap in the well material, the latter corresponding to the lowest energy transition between ground states from hole and electron in wells and $\alpha$ the absorption coefficient. To make valid the application of equation (5) to the radiative coefficient evaluation in wells, the intrinsic carrier concentration and absorption coefficient in wells are calculated

first, considering the presence of discrete energy levels. In particular, the intrinsic carrier concentration at wells is found once the effective density of states of wells is calculated following the procedure reported by Lade and Zahedi [22] and under the Maxwell–Boltzmann approximation to the Fermi–Dirac equation by the following equation:

$$g_{\mathrm{W}} = \frac{m^{*}kT}{\pi\hbar^{2}L_{\mathrm{W}}}\sum_{i}\left[\mathrm{Exp}\left(\frac{-E_{\mathrm{ei}}}{kT}\right) - \exp\left(\frac{-\Delta Ec}{kT}\right)\right] + g_{\mathrm{b}}\left[2\sqrt{\frac{\Delta Ec}{\pi kT}}\exp\left(\frac{-\Delta Ec}{kT}\right) + \mathrm{Erfc}\left(\sqrt{\frac{\Delta Ec}{kT}}\right)\right] \tag{6}$$

where $E_{\mathrm{ei}}$ stands for the energy eigenvalues at wells and Erfc is the error function.

### 2.2. Calculations under nonradiative losses

In the fabrication of solar cells, the introduction of defects could be a limiting factor for achieving efficiencies near the ones expected under the radiative limit. In particular, in QWSCs, defects at interfaces, barriers, and wells could result in device degradation. In this sense, the impact of defects on solar cell efficiency is studied in the last step of this work. For calculations, the influence of defects is evaluated considering the Shockley–Read–Hall recombination theory. In particular, the pessimistic assumption of traps located near the middle of the band-gap and the case of maximum recombination rate that corresponds to similar electron and hole concentrations under nonequilibrium conditions is assumed. Under low injection, the *J*–*V* characteristic of solar cell without nanostructures is given by [19]:

$$J = qWn_{\mathrm{i}}^{2}B\left[\exp\left(\frac{qV}{kT}\right) - 1\right] + \frac{qWn_{\mathrm{i}}}{\tau} \times \left[\exp\left(\frac{qV}{2kT}\right) - 1\right] - J_{\mathrm{PH}} \tag{7}$$

where $\tau$ is the minority carrier lifetime. Following the same pessimistic assumptions for nonradiative losses, the influence of interface, barrier, and well recombinations on QWSC efficiency can be evaluated from the following equation [13]:

$$J_{\mathrm{QWSC}} = qWn_{\mathrm{i}}^{2}B \times \left\{1 + f_{\mathrm{w}}\left[\gamma_{\mathrm{B}}\gamma_{\mathrm{DOS}}^{2}\exp\left(\frac{\Delta Eg - qFL_{\mathrm{W}}}{kT}\right) - 1\right]\right\} \times \left[\exp\left(\frac{qV}{kT}\right) - 1\right] + (J_{0-\mathrm{NR}} + J_{\mathrm{s}}) \times \left[\exp\left(\frac{qV}{2kT}\right) - 1\right] - J_{\mathrm{PH}} \tag{8}$$

where $J_{0\text{-NR}}$ is the reverse dark current density due to nonradiative recombination at barriers and wells and $J_{\mathrm{s}}$ is the reverse dark current density due to recombination at SnS/SnSSe interfaces. These terms are evaluated by the following expressions:

$$J_{0-\mathrm{NR}} = \frac{qWn_{\mathrm{i}}}{\tau}\left\{1 + f_{\mathrm{w}}\left[\gamma_{\mathrm{A}}\gamma_{\mathrm{DOS}}\exp\left(\frac{\Delta Eg - qFL_{\mathrm{W}}}{2kT}\right) - 1\right]\right\} \tag{9}$$

$$J_{\mathrm{s}} = 2qNn_{\mathrm{i}}\gamma_{\mathrm{DOS}}\,v_{\mathrm{s}}\exp\left(\frac{\Delta Eg - qFL_{\mathrm{W}}}{2kT}\right). \tag{10}$$

In equation (9), $\gamma_{\mathrm{A}}$ is the ratio between minority carrier lifetime of wells and barriers, while $v_{\mathrm{s}}$ in equation (10) is the SnS/SnSSe interface recombination speed. For simplicity, we have assumed in calculations similar carrier lifetimes of wells and barriers ($\gamma_{\mathrm{A}} = 1$).

### 2.3. Input parameters and software for evaluation

In order to evaluate QWSC optoelectronic parameters, values of the absorption coefficient as a function of wavelength for bulk material [23], electron and hole effective masses [24], electron affinities [17], and the refractive index [25] were taken from the literature. In addition, a linear direct band-gap variation (a negligible bowing parameter) with Se incorporation between the value of SnSe (1.0 eV) [14, 16] and SnS (1.3 eV) [1, 14] is assumed. Moreover, an electric field value of $4 \times 10^{6}$ V m$^{-1}$ within the absorber region was assumed, as calculated by Poisson's equation for typical SnSSe solar cells. In addition, the AM1.5G solar spectrum (100 mW cm$^{-2}$) is considered.

A package was developed in Wolfram Mathematica version 6.0 to numerically simulate the performance of solar cells without nanostructures as well as the introduction of SnSSe QWs into SnS solar cells. This package contains all the required equations and constants for calculations. It is important to mention that it has been previously used for modeling different types of QWSCs such as GaAs/AlGaAs, GaAs/GaInNAs, and $Cu_2ZnSnS_4$/$Cu_2ZnSn(SSe)_4$ [8, 12, 13]. The *J*–*V* characteristics of solar cells without and with QWs under the radiative limit are evaluated from equations (1) and (2), respectively, while the *J*–*V* characteristics of solar cells without and with QWs with the influence of defects are evaluated by equations (7) and (8), respectively. Once *J*–*V* characteristics as functions of the well properties are known, optoelectronic parameters of solar cells such as $J_{\mathrm{sc}}$, $V_{\mathrm{oc}}$, and efficiency are numerically calculated.

## 3. Results and discussion

The impact of SnS and SnSe absorber thickness on solar cell parameters without the inclusion of QWs was first evaluated and results are presented in figure 2. Maximum efficiency values of 28.9% and 26.1% are expected for SnS and SnSe solar cells, respectively, for thicknesses in the range of 1–2 $\mu$m under the radiative limit. In addition, $J_{\mathrm{sc}}$ values of

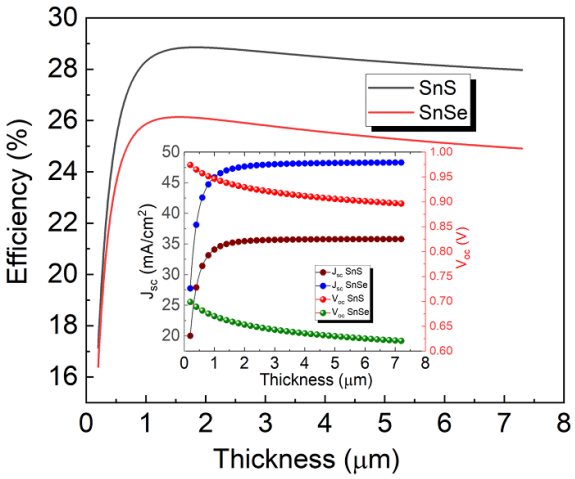



**Figure 2.** SnS and SnSe solar cell efficiencies as functions of the absorber thickness. The inset shows $J_{sc}$ and $V_{oc}$ dependence on the absorber thickness for SnS and SnSe solar cells.

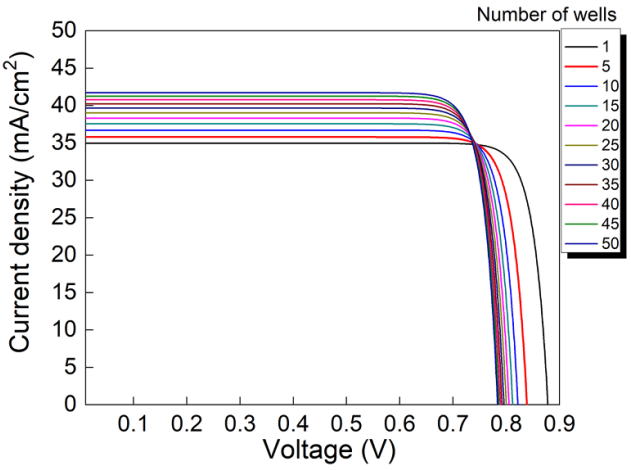



**Figure 3.** *J–V* characteristics of SnS/SnSe quantum well solar cells for different numbers of quantum wells.

35.4 mA cm$^{-2}$ and 47.2 mA cm$^{-2}$ and $V_{oc}$ values of 931.6 mV and 660 mV are found for SnS and SnSe solar cells, respectively, as illustrated in the inset of figure 2. These results are in good agreement with the ones predicted by Shockley–Queisser for these absorber materials [26]. A higher $J_{sc}$ of 47.2 mA cm$^{-2}$ is obtained for SnSe solar cell since a lower band-gap guarantees higher absorption of photons, this value being in good correspondence with the one reported in previous work [27]. From these results, it is observed that the highest efficiency is expected for the SnS solar cell, which is a direct result of the absorber band-gap near the optimal one predicted by Shockley and Queisser [26]. That is, the trade-off between $J_{sc}$ and $V_{oc}$ with band-gap variation results in an optimized efficiency for a band-gap value of 1.3 eV. Therefore, SnS solar cells without QWs are limited to efficiency values lower than 29%. Up to now, SnS solar cells without nanostructures have shown a certified maximum efficiency of 4.36%, with $V_{oc}$, $J_{sc}$, and FF values of 372 mV, 20.2 mA cm$^{-2}$, and 58%, respectively [5], while SnSe solar cells have achieved a maximum efficiency of 6.44% with $V_{oc}$, $J_{sc}$, and FF values of 425 mV, 17.23 mA cm$^{-2}$ and 44%, respectively [28]. A remarkable difference is observed between the experimental and theoretical data for SnS and SnSe solar cells without nanostructures. Taking into account conditions established by the radiative recombination, the difference between experimental and theoretical values could be a direct result of a high defect formation at bulk and interfaces, resulting in a short minority carrier lifetime, low mobility, and consequently short diffusion length of carriers, along with other factors such as non-ideal buffer layer, poor band-alignment, and losses due to reflection and series and shunt resistances as discussed in previous reports [1, 29]. In this sense, further experimental studies focused on improving absorber crystalline quality, the use of an adequate buffer layer, and the reduction of the impact of resistances are needed to achieve efficiency values near the maximum values.

In the next step, the introduction of SnSe QWs into SnS absorber material is evaluated. In particular, an absorber thickness of 1.255 $\mu$m is taken into account, considering that maximum efficiencies for SnS solar cells without QWs are obtained for absorber thicknesses in the range of 1–2 $\mu$m, as shown in figure 2. For calculations, a well thickness of 20 nm is initially considered so that up to 50 wells can be embedded into SnS absorber material, to avoid the device degradation due to interface recombination for a higher number of wells as experimentally reported for other QWSCs [10, 30]. Under these conditions, the lowest barrier thickness would be 5 nm, for which initial calculations show that there is no coupling effect between wells, and hence the structure can be considered as multiple QWs instead of a superlattice. The impact of SnSe QW number on *J–V* characteristics is illustrated in figure 3, where a range of 1–50 wells is taken into account. The inclusion of SnSe QWs into SnS solar cells provides an increase in the $J_{sc}$ of the device due to the higher absorption of photons. That is, the higher number of wells the larger absorption of photons with energies lower than the SnS band-gap will be, resulting in an enhanced $J_{sc}$ as illustrated in figure 3. On the contrary, the voltage output of the solar cell is reduced with the QW number increasing due to an increase of carrier recombination. In other words, the increase in QW number not only allows a higher photogeneration of electron–hole pairs but also the increase in recombination due to the confinement of carriers within wells.

A detailed analysis of the behavior of optoelectronic parameters with the well number is presented in figure 4. Results on optoelectronic parameters of SnS and SnSe solar cells without QWs and with the same thickness are also illustrated for comparison. Figure 4(a) shows the dependence of $J_{sc}$ on the well number. $J_{sc}$ values in the range of 35–42 mA cm$^{-2}$ are found. It is remarked that $J_{sc}$ values for SnS/SnSe QWSCs are between values obtained for SnS and SnSe solar cells without QWs. Particularly, $J_{sc}$ values higher than that of optimized SnS solar cell are displayed, which demonstrates the ability of the proposed structure to achieve higher absorption of photons.

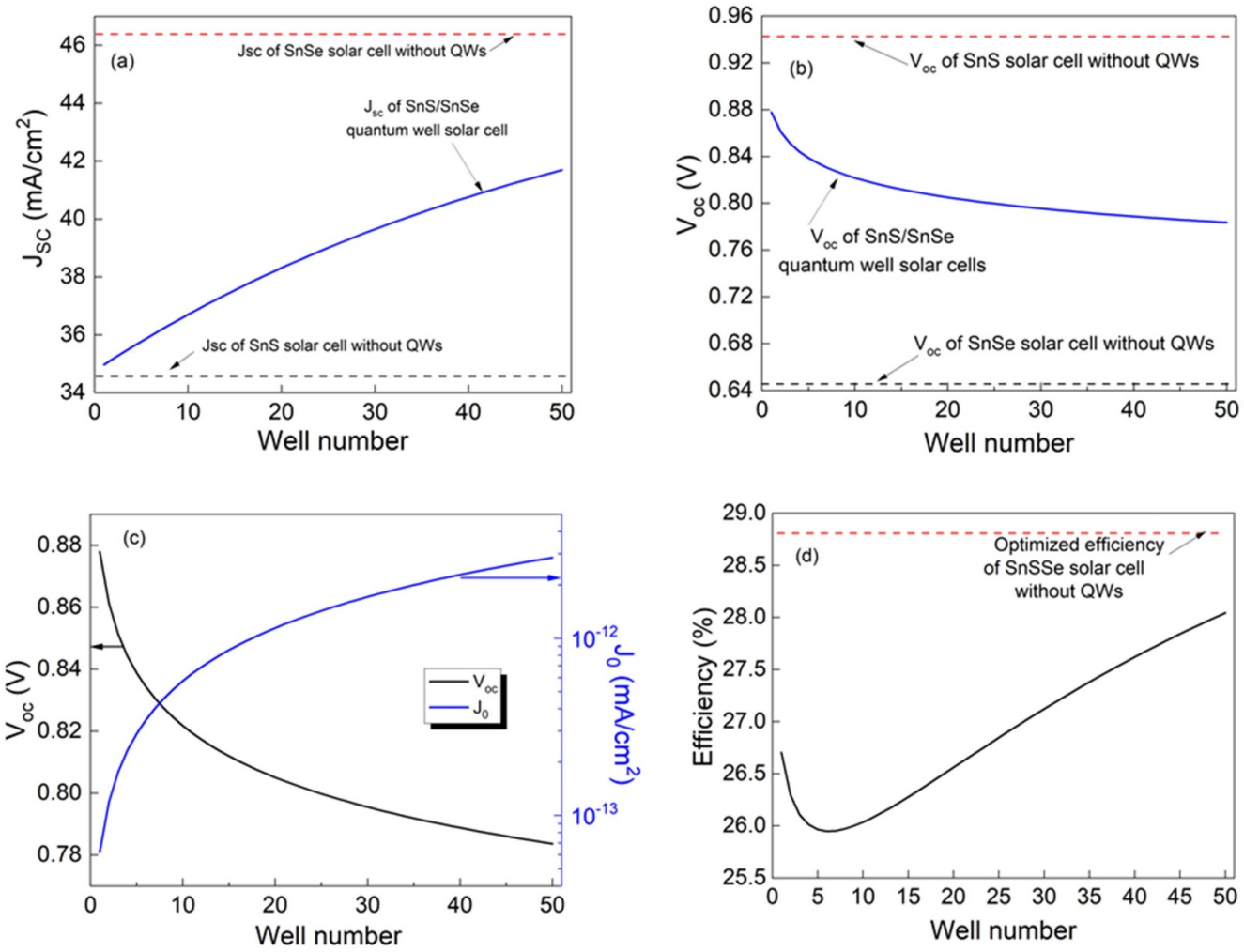



**Figure 4.** Impact of well number on *J*sc (a), *V*oc (b), *V*oc and $J_0$ (c), and efficiency (d) in SnS solar cells with the incorporation of SnSe quantum wells. Optoelectronic parameters of SnS and SnSe solar cells without QWs are added for comparison.

Besides, it is illustrated that for the inclusion of a single well, $J_{sc}$ is nearly the value of the optimized SnS solar cell without wells. In addition, $J_{sc}$ values are lower than that of optimized SnSe solar cell as expected. The impact of SnSe QW number on $V_{oc}$ is presented in figure 4(b), where a decrease from 0.88 to 0.78 V is found with the well number increasing from 1 to 50. The decrease of $V_{oc}$ is a direct result of the carrier recombination increase and thereby the reverse dark current density ($J_0$), as presented in figure 4(c). In particular, the $V_{oc}$ is drastically reduced with the well number increasing from 1 to 10 since $J_0$ increases one order of magnitude as supported by equation (2). It is pointed out that $V_{oc}$ values lower than that of optimized SnS solar cell are illustrated, emphasizing the increase of carrier recombination due to the inclusion of wells. However, it is noted that the $V_{oc}$ of SnS/SnSe QWSCs is higher than that of the optimized SnSe solar cell, which is characterized by a lower band-gap and hence a reduced $V_{oc}$. The dependence of solar cell efficiency on well number is shown in figure 4(d), where the maximum efficiency of SnS solar cell without QW is presented for comparison. A reduction of solar cell efficiency is observed with the increase of well number from 1 to 5, as a result of the introduction of few wells, where carrier generation rate is not able to overcome carrier recombination rate. On the contrary, for a well number higher than 5, solar cell efficiency increases with the well number increase. In particular, a maximum solar cell efficiency of 28% is found for 50 wells of 20 nm width, being this efficiency value lower than the maximum obtained for the optimized SnS solar cell. These results demonstrate that the introduction of 50 wells of 20 nm width of SnSe into SnS solar cells does not favor efficiencies higher than that of the optimized SnS solar cell without QWs. That is, the absorption of extra photons with the introduction of deep wells is not able to overcome carrier recombination due to the confinement of carriers.

The role of different well thicknesses is now evaluated. The formation of energy levels within SnSe wells for different well thicknesses is studied and results are presented in figure 5. The formation of up to six discrete levels for electrons in well is illustrated for a well thickness of 20 nm. For narrow wells, a lower number of energy levels is shown, which are energetically quite separated from the bottom of well, due to carrier confinement in wells. With the increase of well thickness, there is an increase in energy levels as well as a shift of energy levels

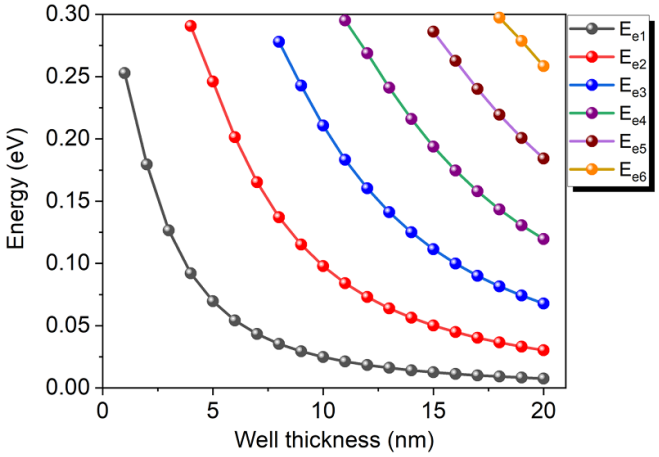



**Figure 5.** Energy level positions at SnSe wells as functions of SnSe well thickness.

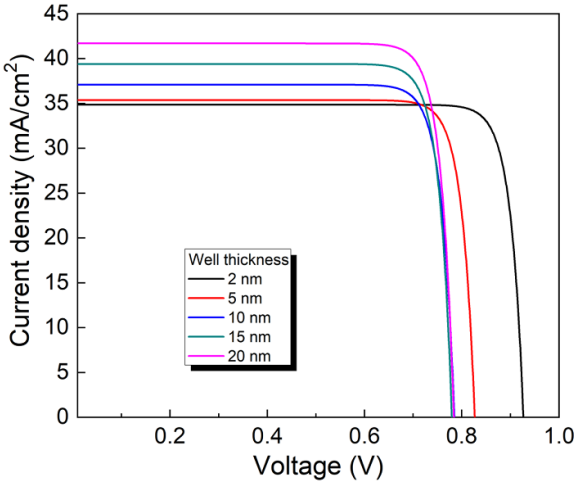



**Figure 6.** *J*–*V* characteristics of SnS/SnSe quantum well solar cells for different thicknesses of quantum wells.

towards lower energy values, which is in good correspondence with quantum mechanics' results. As a consequence, the absorption at wells can be tailored dependent on well thickness.

The *J*–*V* characteristics of SnS/SnSe QWSCs for different well thicknesses are calculated. For calculations, a maximum number of 50 wells of SnSe is considered. Figure 6 shows *J*–*V* characteristics of SnS/SnSe QWSCs with well thicknesses of 2, 5, 10, 15, and 20 nm. A higher $J_{sc}$ is observed with the well thickness increase, which is a result of a higher photon absorption through the formation of new energy levels and their shift toward lower energies as shown in figure 5. On the contrary, a reduction of $V_{oc}$ is also found with well thickness increase, due to a higher population of carriers in wells, thereby enhancing carrier recombination. The behavior of optoelectronic parameters with well thickness is presented in figure 7. Optoelectronic parameters of SnS and SnSe solar cells without QWs with the same thickness are added for comparison. Figure 7(a) shows the effect of well thickness on $J_{sc}$. An increase in $J_{sc}$ from 35 mA cm$^{-2}$ to 42 mA cm$^{-2}$ is found with the well thickness increasing from 1 nm to 20 nm. It is worth noting that narrow wells provide similar $J_{sc}$ values to the one obtained for the SnS solar cell with the same thickness but without nanostructures. This result is explained considering that for narrow wells the absorption of photons is limited to one or two energy levels in the best case, as displayed in figure 5. The maximum $J_{sc}$ is achieved for wells of 20 nm width, this value being lower than the one obtained in SnSe solar cells with the same thickness but without QWs, as expected. The drop in $V_{oc}$ with well thickness increasing from 1 nm to 10 nm is illustrated in figure 7(b). This trend is a direct consequence of the $J_0$ increment, as shown in figure 7(c). The increase in well thickness favors the formation of a higher number of energy levels, as demonstrated in figure 5, and consequently a higher concentration of carriers in wells, thereby increasing carrier recombination. However, for a well thickness greater than 10 nm, $J_0$ and $V_{oc}$ are nearly constant since carriers are able to escape from wells with the help of the electric field. The effect of well thickness on solar cell efficiency is shown in figure 7(d). The well thickness variation from 1 nm to 8 nm results in an efficiency drop, which is due to the fact that extra generation of electron–hole pairs is not able to overcome losses due to carrier recombination. Since $V_{oc}$ is nearly the same for well thicknesses greater than 8 nm, improvement in solar cell efficiency is expected with well thickness enlargement, as presented in figure 7(d). It is pointed out that under the conditions of 50 wells of SnSe embedded within SnS material, solar cell efficiency is not able to overcome the optimized value obtained for the SnS solar cell.

Another important parameter to be studied is the impact of Se composition at wells. The formation of energy levels within SnSSe wells for different Se/(S + Se) compositional ratios is now studied. Figure 8 shows results on energy levels position for a QW thickness of 20 nm. The presence of discrete levels in the well is observed for all Se/(S + Se) compositional ratios. A higher number of energy levels is illustrated for higher Se composition, which is a result of the increase in well depth. In particular, when SnSe is used as the well material, the greatest well depth is obtained (0.3 eV), being characterized by the formation of six energy levels at the well, which is in good correspondence with our previous results. Therefore, up to six energy levels at wells will be governing the solar cell characteristics with the variation of Se/(S + Se) compositional ratio at wells. Another interesting feature is that the first two energy level positions are nearly the same with Se concentration increasing, which is in good correspondence with quantum mechanics' results on wells with infinite barriers—for deep wells the lowest energies are independent of well depth, resembling the case of infinite barriers.

The influence of the Se/(S + Se) compositional ratio at wells on the *J*–*V* characteristics of SnS/SnSe QWSCs is studied. For calculations, 50 wells of 20 nm width are considered. The *J*–*V* characteristics of SnS/SnSe QWSCs with Se/(S + Se) compositional ratios at wells of 0.2, 0.4, 0.6, 0.8 and 1 are presented in figure 9. With the increase in Se/(S + Se) compositional ratio, deeper wells are obtained, which results in higher photon absorption due to the formation of a higher number

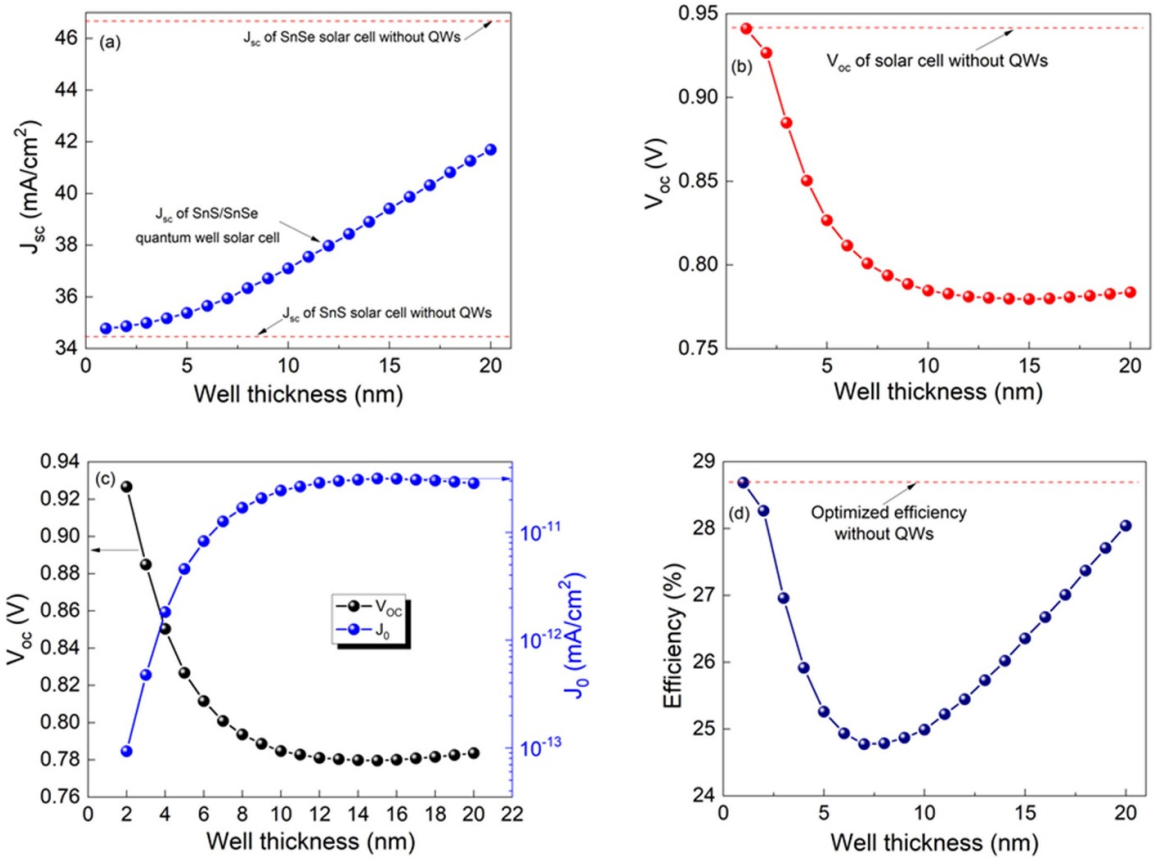



**Figure 7.** Impact of well thickness on $J_{sc}$ (a), $V_{oc}$ (b), $V_{oc}$ and $J0$ (c), and efficiency (d) in SnS solar cells with the incorporation of SnSe quantum wells. Optoelectronic parameters of SnS and SnSe solar cells without QWs are added for comparison.

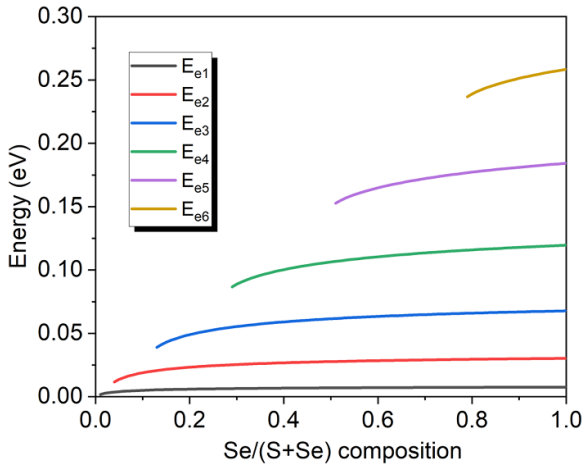



**Figure 8.** Energy level positions at SnSSe wells as functions of Se/(S + Se) compositional ratio.

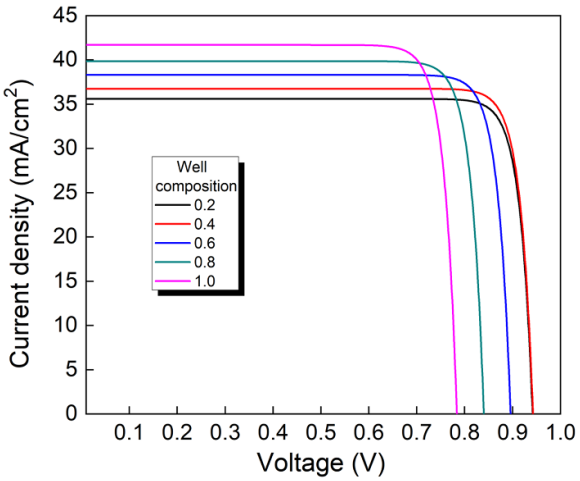



**Figure 9.** *J*–*V* characteristics of SnS/SnSe quantum well solar cells for different Se/(S + Se) compositional ratios at quantum wells.

of energy levels at wells, as previously shown in figure 8. In this sense, a higher $J_{sc}$ is obtained with the increase in the Se/(S + Se) compositional ratio. As a general trend, $V_{oc}$ is reduced with the Se/(S + Se) compositional ratio increasing from 0.2 to 1, since carriers are more confined at wells and hence carrier recombination increases. In order to better understand the role of the Se/(S + Se) compositional ratio on solar cell parameters, a detailed study of optoelectronic parameters is presented in figure 10. Device parameters for SnS and SnSe solar cells without QWs with the same thickness are added for comparison. The $J_{sc}$ increases from 35 mA cm$^{-2}$ to 42 mA cm$^{-2}$ with the Se/(S + Se) compositional ratio

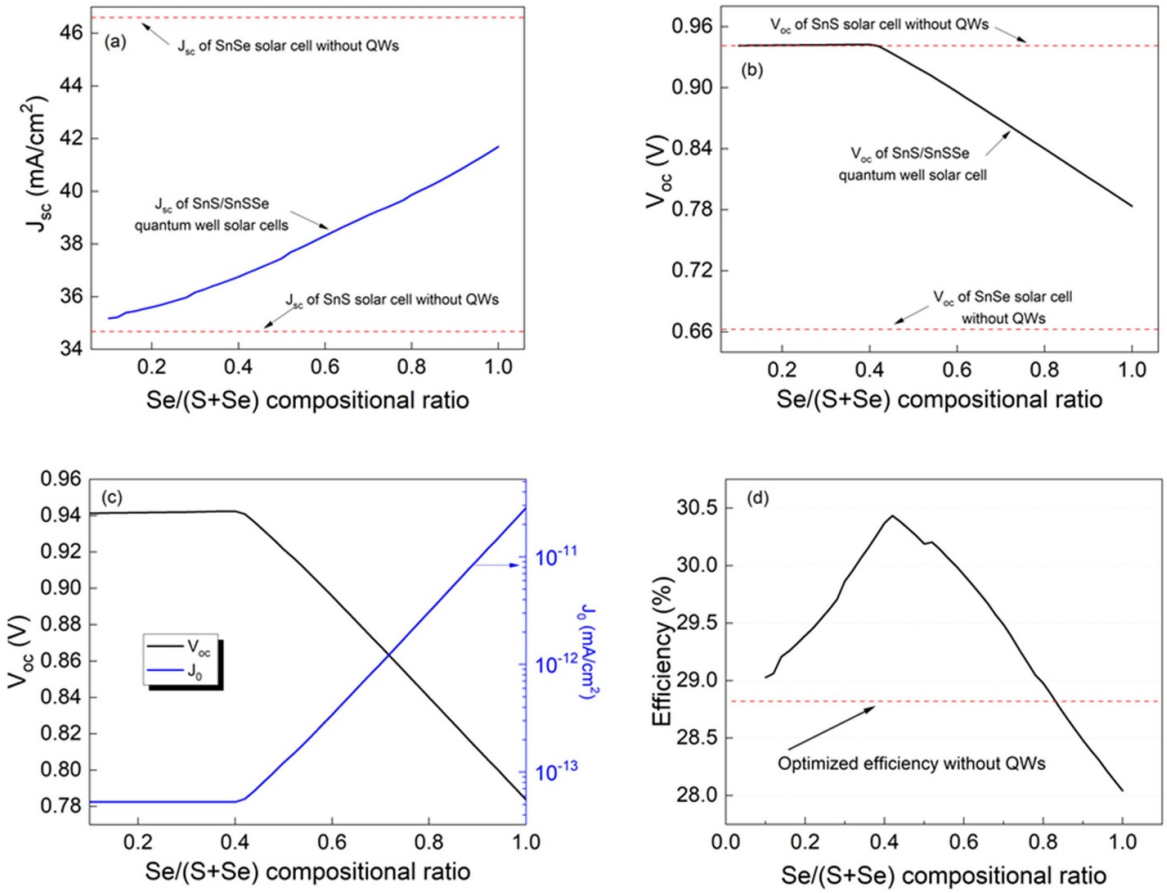



**Figure 10.** Impact of Se/(S + Se) compositional ratio on $J_{sc}$ (a), $V_{oc}$ (b), $V_{oc}$ and $J_0$ (c), and efficiency (d) in SnS solar cells with the incorporation of SnSSe quantum wells. Optoelectronic parameters of SnS and SnSe solar cells without QWs are added for comparison.

increasing from 0.1 to 1, as illustrated in figure 10(a). Particularly, for the lowest Se/(S + Se) compositional ratios, shallow wells with few energy levels are obtained, limiting the absorption of photons, which results in $J_{sc}$ values that are similar to those for the SnS solar cell with the same thickness, but without QWs. For a Se/(S + Se) compositional ratio of 1, which corresponds to the SnSe material at wells, results are in good agreement with the ones obtained in our previous calculations (figures 4 and 7). Results for $V_{oc}$ as a function of Se/(S + Se) compositional ratio are presented in figure 10(b). $V_{oc}$ is almost constant for Se/(S + Se) compositional ratios lower than 0.42. In particular, this value is equal to the one obtained for the SnS solar cell with the same thickness but without QWs. This result can be explained considering that in shallow wells, carriers are likely to escape with the help of the electric field. In this sense, the $V_{oc}$ behavior is dominated by the bulk SnS material. Nevertheless, for Se/(S + Se) compositional ratios higher than 0.42, a decrease in $V_{oc}$ is demonstrated due to the well depth enlargement, which favors the increase in carrier confinement at wells, and consequently their recombination. The behavior of $V_{oc}$ with the Se/(S + Se) compositional ratio is a direct result of the dependence of $J_0$ on the Se/(S + Se) compositional ratio, as displayed in figure 10(c). The trade-off between $V_{oc}$ and $J_{sc}$ provides a particular trend for solar cell efficiency, as presented in figure 10(d). Solar cell efficiency increases as the Se/(S + Se) compositional ratio increases from 0.1 to 0.4, since with the increase in Se concentration until 0.4, up to four energy levels are formed (figure 8). As a result, there is a greater absorption of photons, which promotes $J_{sc}$ while $V_{oc}$ is nearly constant. For a Se/(S + Se) compositional ratio higher than 0.4, efficiency is reduced since carrier recombination overcomes carrier generation. That is, photogenerated carriers are less likely to escape from deep wells, resulting in a higher recombination rate. It is important to remark that efficiencies higher than that of optimized SnS solar cells with the same thickness, but without QWs, are achieved for Se/(S + Se) compositional ratios lower than 0.8. Therefore, unlike our previous results, it is demonstrated that the addition of SnSSe QWs into SnS solar cells can be a route to increase device efficiency. In particular, a maximum efficiency of 30.4% can be attained for a Se/(S + Se) compositional ratio at wells near 0.4.

For the next calculations, the simultaneous effect of two well parameters on device properties is evaluated for a better understanding of the role that is played by the introduction of SnSSe wells in SnS solar cells. The impact of different Se/(S + Se) compositional ratios at wells and well numbers on efficiency, $J_{sc}$ and $V_{oc}$ is presented in figure 11. As a general trend, the efficiency is increased as the well number increases up to 50 wells, which is a result of the higher

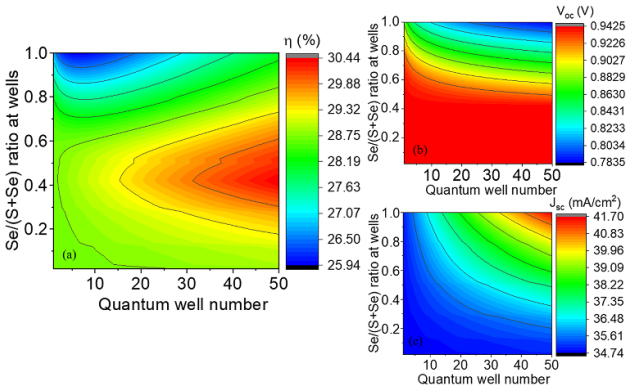



**Figure 11.** Impact of Se/(S + Se) well composition and SnSSe well number on efficiency (a), $V_{oc}$ (b), and $J_{sc}$ (c) of SnS solar cells with the incorporation of SnSSe quantum wells.

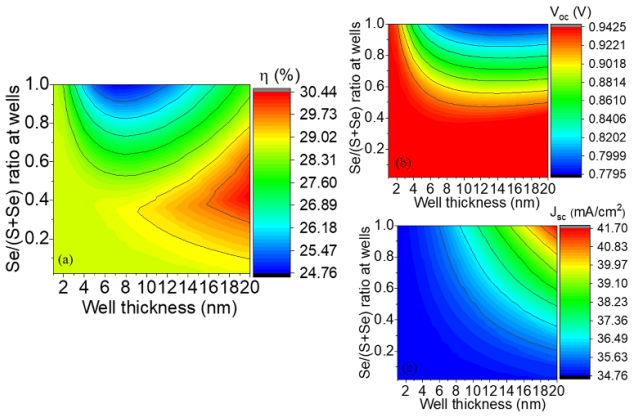



**Figure 12.** Impact of Se/(S + Se) well composition and SnSSe well thickness on efficiency (a), $V_{oc}$ (b), and $J_{sc}$ (c) of SnS solar cells with the incorporation of SnSSe quantum wells.

photon absorption, as mentioned before. Therefore, for further calculations, the number of wells can be set to 50. A trade-off between $J_{sc}$ and $V_{oc}$ is observed, where the increase in Se/(S + Se) well composition leads to an increase in $J_{sc}$ due to higher absorption of photons as well as a decrease in $V_{oc}$, as a result of higher carrier recombination—carriers are less likely to escape from deep wells, thereby increasing recombination losses. As a result of this trend, efficiencies are optimized for QWs with Se/(S + Se) compositions in the range of 0.3–0.6, which correspond to neither shallow nor deep wells. Moreover, it is pointed out that the use of SnSSe QWs in SnS solar cells can result in efficiencies higher than that of the optimized devices without QWs, for a well number higher than 30 and Se/(S + Se) compositions near 0.4. In particular, a solar cell efficiency of about 30.4% is expected. The effect of introducing QWs is also observed when comparing $J_{sc}$ and $V_{oc}$ from figure 11 with the maximum results obtained for the optimized SnS and SnSe solar cells. That is, for 50 wells with Se/(S + Se) compositions of about 0.4, the $V_{oc}$ is mainly described by the SnS solar cell, while $J_{sc}$ is higher than the one obtained for the optimized SnS solar cell. In this sense, the introduction of SnSSe QWs into SnS solar cells can promote efficiency from 28.9% to 30.4%.

The impact of well thickness and Se/(S + Se) well composition on efficiency, $J_{sc}$, and $V_{oc}$ was studied, and results are presented in figure 12. For calculations, an absorber thickness of 1.255 $\mu$m and 50 wells with thicknesses in the range of 2–20 nm were assumed so that a minimum barrier thickness of 5 nm is obtained. Greater $J_{sc}$ values are observed with the increase in well thickness and depth. This is a consequence of the higher absorption of photons while $V_{oc}$ is reduced since carriers are unable to escape from deep wells. It is interesting to note that $V_{oc}$ is mostly characterized by the value of the SnS solar cell without QWs for Se/(S + Se) well compositions lower than 0.5. As a result, Se/(S + Se) well compositions of about 0.4 provide the greatest efficiency values for thicknesses larger than 16 nm. The maximum efficiency of 30.4% is expected for 50 wells with the highest thickness (20 nm) and a Se/(S + Se) compositional ratio of 0.4, which is in good correspondence with our previous results.

The use of either a higher well thickness or a higher well number is required to further increase device efficiency. A higher number of wells can result in device degradation due to the introduction of interface recombination, as experimentally reported for other QWSCs [10, 30]. Therefore, the option of tailoring the well thickness is further considered. In order to evaluate the impact of well thicknesses larger than 20 nm, the absorber thickness should be changed, but keeping the previous conditions of 50 wells, barrier thicknesses of 5 nm, and an optimized well composition of 0.4. From figure 2, it can be seen that an absorber thickness variation from 1.255 $\mu$m up to 7.255 $\mu$m results in an efficiency reduction of less than 1%. In this sense, the impact of absorber thickness (in the range of 1.255–7.255 $\mu$m) on device parameters can be neglected. The influence of well thicknesses in the range of 20–140 nm on efficiency, $J_{sc}$, and $V_{oc}$ is presented in figure 13. To perform calculations, absorber thickness is varied so that a minimum barrier thickness of 5 nm between the 50 wells is kept constant. As a consequence of absorber thickness variation, the electric field value is linearly reduced as thickness increases. Higher photon absorption is obtained for well thicknesses greater than 20 nm, resulting in an increased $J_{sc}$ and thereby the efficiency increase. However, for well thicknesses greater than 60 nm, the complete absorption of photons is almost reached and then the efficiency is reduced due to $V_{oc}$ reduction, as shown in the inset of figure 13. The maximum efficiency of 32.1% is expected for QW thicknesses near 54 nm, which corresponds to $J_{sc}$ and $V_{oc}$ values of 40.55 mA cm$^{-2}$ and 905.8 mV, respectively. The advantage of using QWs in SnS solar cells is noted when comparing these results with the one obtained for the optimized SnS solar cell without QWs. In particular, solar cell efficiency is 11.1% higher than the maximum expected for SnS solar cell without QWs, which is a result of the increase of $J_{sc}$ by 14.5% due to higher absorption of photons, while $V_{oc}$ is only decreased by 2.8%. In other words, the introduction of 50 wells of 54 nm width with a Se/(S + Se) well composition of about 0.4 into the SnS solar cell allows us to retain $V_{oc}$ values near the optimal one of the bulk cell while $J_{sc}$ is increased, thereby increasing solar cell efficiency.

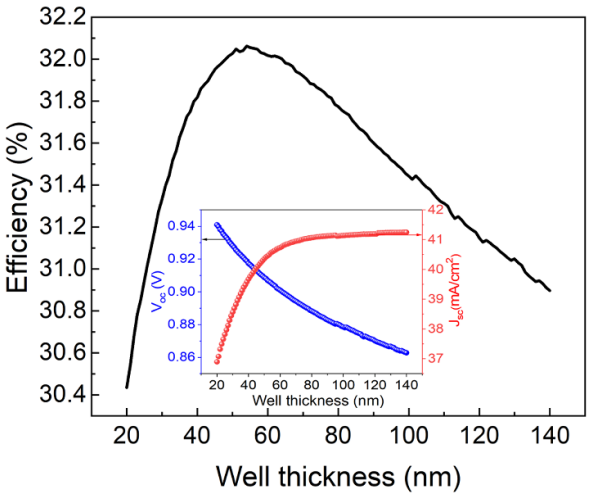



**Figure 13.** Efficiency as a function of well thickness for SnS solar cell, considering 50 wells with Se/(S + Se) composition of 0.4. Results on $V_{oc}$ and $J_{sc}$ as functions of well thickness are shown in the inset.

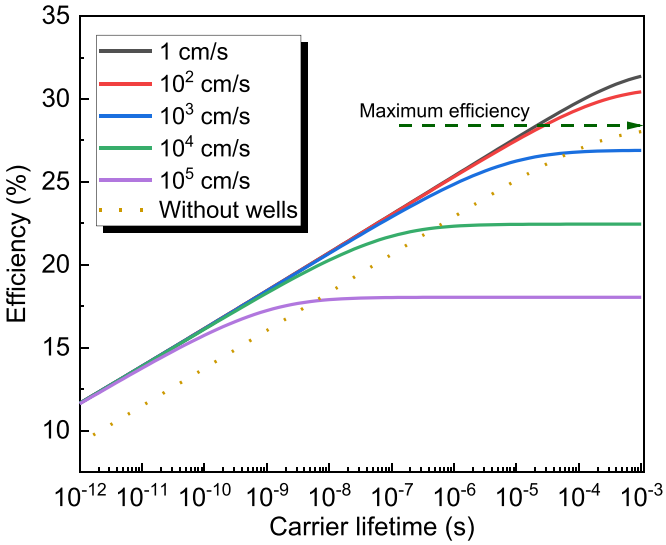



**Figure 14.** Influence of barriers and wells minority carrier lifetime and $SnS/SnS_{0.6}Se_{0.4}$ interface recombination speed on quantum well solar cell efficiency. The impact of minority carrier lifetime on the optimized SnS solar cell without quantum wells is also added for comparison.

Previous results were obtained under the radiative limit; however, the introduction of defects could have a larger detrimental effect than the calculated gain. In this sense, the influence of defects at wells and barriers through the minority carrier lifetime and at the $SnS/SnS_{0.6}Se_{0.4}$ interface through the interface recombination speed was evaluated in the last step. For calculations, minority carrier lifetime values in the range of 1 ps–1 ms and interface recombination speed values in the range of 1–$10^5$ cm s$^{-1}$ were assumed. Results are presented in figure 14, where the dependence of SnS solar cell efficiency on minority carrier lifetime for the optimized device without QWs is also illustrated for comparison. Figure 14 shows that an efficiency value of less than 10% is expected for SnS solar cells without nanostructures for a minority carrier lifetime of only a few picoseconds, as experimentally reported [31]. If other factors such as resistances and a non-ideal buffer layer were considered, efficiency would be in good agreement with the experimentally reported values elsewhere. On the other hand, in order to achieve QWSC efficiency values higher than the maximum expected for the optimized SnS solar cell without QWs, minority carrier lifetimes of longer than 10 $\mu$s and interface recombination speed values lower than $10^3$ cm s$^{-1}$ are needed. A low recombination speed value at the $SnS/SnS_{0.6}Se_{0.4}$ interface is experimentally expected due to the similar lattice constants between SnS and $SnS_{0.6}Se_{0.4}$; however, the good crystalline quality of materials resulting in a low formation of defects is required to achieve minority carrier lifetimes that are longer than 10 $\mu$s. For minority carrier lifetime values of less than 10 $\mu$s and interface recombination speed values higher than $10^3$ cm s$^{-1}$, the efficiency of QWSCs is lower than the optimized SnS solar cell without QWs. However, it is important to point out that QWSC efficiency can be higher than the efficiency of the device without QWs as shown in figure 14. That is, for interface recombination speed values of $10^3$, $10^4$, and $10^5$ cm s$^{-1}$, minority carrier lifetimes lower than 60 $\mu$s, 0.5 $\mu$s, and 6 ns, respectively result in QW solar cell efficiencies higher than the one of the devices without QWs. This is a result of the higher absorption of photons in QWSCs in comparison to the device without QWs when bulk defects are dominant. However, with the increase in minority carrier lifetime, an important aspect to consider is the effect of high interface recombination speed values, which can reduce QWSC efficiency to values lower than the ones obtained in solar cells without QWs. Nevertheless, it is important to remark that there is a slight variation in lattice parameters from SnS ($a$ = 3.98 Å, $b$ = 4.52 Å and $c$ = 11.16 Å) to SnSe ($a$ = 4.16 Å, $b$ = 4.61 Å and $c$ = 11.54 Å) [1, 16]. In this sense, defect formation at the $SnS/SnS_{0.6}Se_{0.4}$ interface is expected to be low and, consequently, the introduction of QWs should result in higher solar cell efficiencies in comparison to the device fabricated under the same conditions but without QWs. As a result, the use of SnSSe QWs in SnS solar cells constitutes a route to achieve efficiency values that are higher than the experimentally reported ones for traditional SnS solar cells.

In order to achieve efficiencies higher than 29%, it is important to consider that SnSSe material should be deposited by a technique that guarantees a fine control of composition, very thin layers, and a negligible contribution of defects at barriers, wells (high crystalline quality) and interfaces. The molecular beam epitaxy (MBE) technique is known to fulfill all these requirements. Deposition rates of about 1 Å s$^{-1}$ have been reported by the MBE technique, which makes it possible to obtain very thin barriers of 5 nm between wells and the required composition while keeping the adequate crystalline quality [32, 33].

## 4. Summary

In summary, a theoretical study on the introduction of SnSSe QWs into SnS solar cells under the radiative limit is presented for the first time. The addition of SnSSe QWs into SnS solar cells is presented as a potential route to achieving higher efficiencies than the ones obtained in traditional SnS solar cells due to the higher absorption of photons. In particular, an efficiency promotion of 11.1% is expected in comparison to the optimized solar cell without QWs, by embedding 50 wells of 54 nm width with a Se/(S + Se) well composition of 0.4 into the SnS solar cell. The impact of defects on devices was studied in a further step. We found that an efficiency increase for QWSCs in comparison to the optimized device without QWs can only be obtained for minority carrier lifetimes that are longer than 10 $\mu$s and interface recombination speed values lower than $10^3$ cm $s^{-1}$. However, it was demonstrated that the introduction of QWs results in a higher solar cell efficiency in comparison to the device without QWs. Therefore, this work presents a potential route to increase SnS solar cell efficiency, which can be extended to quantum dots or other nanostructures.

## Data availability statement

The data that support the findings of this study are available upon reasonable request from the authors.

## Acknowledgments

M Courel acknowledges financial support under project PRODEP-NPTC (UDG-PTC-1523) and PRO-SNI from the University of Guadalajara. P Beltrán-Bobadilla and A Carrillo-Osuna acknowledge fellowship support from CONACyT for masters degree study. LMP and DL acknowledge partial financial support from FONDECYT 1180905. DL acknowledges partial financial support from Centers of excellence with BASAL/CONICYT financing, AFB 180001, CEDENNA.

## ORCID iDs

Maykel Courel https://orcid.org/0000-0001-9149-3506
I Montoya De Los Santos https://orcid.org/0000-0003-3664-1881
D Laroze https://orcid.org/0000-0002-6487-8096
E Feddi https://orcid.org/0000-0001-6641-3623

## References

[1] Andrade-Arvizu J A, Courel-Piedrahita M and Vigil-Galán O 2015 *J. Mater. Sci., Mater. Electron.* **26** 4541–56
[2] Reddy K T R, Reddy N K and Miles R W 2006 *Sol. Energy Mater. Sol. Cells* **90** 3041–6
[3] Noguchi H, Setiyadi A, Tanamura H, Nagatomo T and Omoto. O 1994 *Sol. Energy Mater. Sol. Cells* **35** 325–31
[4] Spalatu N, Hiie J, Kaupmees R, Volobujeva O, Krustok J, Acik I O and Krunks M 2019 *ACS Appl. Mater. Interfaces* **11** 17539–54
[5] Sinsermsuksakul P, Sun L, Woon Lee S, Hejin Park H, Bok Kim S, Yang C and Gordon R G 2014 *Adv. Energy Mater.* **4** 1400496
[6] Cho J Y *et al* 2020 *J. Mater. Chem.* A **8** 20658–65
[7] Yun H-S, Park B-W, Choi Y C, Im J, Shin T J and Seok S I 2019 *Adv. Energy Mater.* **9** 1901343
[8] Courel. M 2019 *Appl. Phys. Lett.* **115** 123901
[9] Sayed I E H, Jain N, Steiner M A, Geisz J F and Bedair. S M 2017 *Appl. Phys. Lett.* **111** 082107
[10] Sayed I and Bedair S M 2019 *IEEE J. Photovoltaics* **9** 402–23
[11] Barnham K W J and Duggan G 1990 *J. Appl. Phys.* **67** 3490
[12] Courel M, Rimada J C and Hernández. L 2012 *J. Appl. Phys.* **112** 054511
[13] Courel M, Rimada J C and Hernández L 2013 *Prog. Photovoltaics Res. Appl.* **21** 276–82
[14] Parenteau M and Carlone. C 1990 *Phys. Rev.* B **41** 5227
[15] Meza-Avendaño C A, Courel M, Pantoja-Enríquez J, Castañeda-Valderrama R, Martínez Ayala A, Montoya De Los Santos I and Borrego-Pérez J A 2019 *Mater. Res. Express* **6** 076413
[16] Bindu K and Nair P K 2004 *Semicond. Sci. Technol.* **19** 1348–53
[17] Im H S *et al* 2013 *RSC Adv.* **3** 10349–54
[18] Ramasamy P, Manivasakan P and Kim J 2015 *Cryst. Eng. Comm.* **17** 807–13
[19] Jiménez T, Seuret-Jiménez D, Vigil-Galán O, Basurto-Pensado M A and Courel M 2018 *J. Phys. D: Appl. Phys.* **51** 435501
[20] Bastard G 1988 *Wave Mechanics Applied to Semiconductor Heterostructures* (Les Ulis: Les Editions de Physique)
[21] Nelson J, Paxman M, Barnham K W J, Roberts J S and Button C 1993 *IEEE J. Quantum Electron.* **29** 1460–8
[22] Lade S J and Zahedi. A 2004 *Microelectron. J.* **35** 401–10
[23] Minbashi M, Ghobadi A, Ehsani M H, Rezagholipour Dizaji H and Memarian N 2018 *Sol. Energy* **176** 520–5
[24] Tritsaris G A, Malone B D and Kaxiras E 2013 *J. Appl. Phys.* **113** 233507
[25] Safak H, Merdan M and Yuksel. O F 2002 *Turk. J. Phys.* **26** 341–7
[26] Shockley W and Queisser H J 1961 *J. Appl. Phys.* **32** 510
[27] Ruhle S 2016 *Sol. Energy* **130** 139–47
[28] Abd El-Rahman K F, Darwish A A A and El-Shazly E A A 2014 *Mater. Sci. Semicond. Process.* **25** 123–9
[29] Beltrán-Bobadilla P, Carrillo-Osuna A, Rodriguez-Valverde J A, Acevedo-Juárez B, Montoya De Los Santos I, Sánchez-Rodriguez F J and Courel M 2021 *Gen. Chem.* **7** 200012
[30] Bushnell D B, Tibbits T N D, Barnham K W J, Connolly J P, Mazzer M, Ekins-Daukes N J, Roberts J S, Hill G and Airey R 2005 *J. Appl. Phys.* **97** 124908
[31] Jaramillo R, Sher M-J, Ofori-Okai B K, Steinmann V, Yang C, Hartman K, Nelson K A, Lindenberg A M, Gordon R G and Buonassisi T 2016 *J. Appl. Phys.* **119** 035101
[32] Curé Y, Pouget S, Reita V and Boukari. H 2017 *Scr. Mater.* **130** 200–4
[33] Song N, Young M, Liu F, Erslev P, Wilson S, Harvey S P, Teeter G, Huang Y, Hao X and Green. M A 2015 *Appl. Phys. Lett.* **106** 252102